ZIBELINE INTERNATIONAL™ PUBLISHING

ISSN: 2521-294X (Online)
ISSN: 2521-2931 (Print)
CODEN: MJSAEJ

Malaysian Journal of Sustainable Agriculture (MJSA)

DOI: http://doi.org/10.26480/mjsa.02.2026.39.44

RESEARCH ARTICLE

VALORIZATION OF RICE HUSK LIGNOCELLULOSE VIA MICROWAVE-ASSISTED FURAN FUNCTIONALIZATION AND ITS CORROSION INHIBITION ON STAINLESS STEEL 304L

Paler, K.M.S*., Quimque, M.T.J., Bendoy, A.P.

Department of Chemistry, College of Science and Mathematics, Mindanao State University, Iligan Institute of Technology, A. Bonifacio Ave. Tibanga, Iligan City, Philippines, 9200
Corresponding Author Email: karlmichael.paler@g.msuiit.edu.ph

ARTICLE DETAILS

Article History:

Received 15 October 2025
Revised 19 November 2025
Accepted 20 December 2025
Available online 05 February 2026

ABSTRACT

Lignin-based corrosion barriers have gained interest among researchers due to the abundance, low-cost and film-forming ability of lignin. However, previous studies have used petroleum-based synthetic polymer composites, thereby introducing environmental concerns. Herein, microwave irradiation was utilized to functionalize rice husk-derived lignin with furanic groups for corrosion protection of SUS304L stainless steel. Lignin was extracted using a deep eutectic solvent (DES) choline chloride-*p*-toluenesulfonic acid mixture, before further modification. Results showed the successful introduction of furan moieties into the lignin structure, which is substantiated by the increase in oxygen-rich functional groups in the pyrolysis data. From the electrochemical tests in 3.5% NaCl, the functionalized lignin coatings (fRH-L) exhibited significantly lower current density of 2.7 nA·cm^{-2}, leading to 99% inhibition efficiency as compared to 190.2 nA·cm^{-2} for bare SUS304L stainless steel. Furthermore, impedance modeling revealed enhanced dielectric properties and reduced capacitance. These results strongly suggest that the prepared functionalized DES-extracted lignin exhibits a noteworthy improvement in corrosion resistance compared to pure lignin (RH-L) and bare SUS304L stainless steel. Although degradation occurred after 24 hours, fRH-L coatings retained superior protection compared to unmodified lignin. This study highlights the potential of rice husk lignin as a sustainable, corrosion barrier through biomass valorization using DES and microwave irradiation techniques.

KEYWORDS

Green Functionalization, Lignin, Corrosion Resistance, Deep Eutectic Solvent, Microwave

1. INTRODUCTION

Stainless steel such as SUS304L is widely used in crude oil processing, manufacturing, transportation, and construction due to its favorable mechanical properties and cost-effectiveness (Baddoo, 2008 ; Haruna and Saleh, 2022). The SUS304L stainless steel contains chromium which forms an oxide layer that prevents corrosion (Loto, 2019). However, its electrochemical reactivity makes it susceptible to corrosion in saline and acidic environments, posing significant economic and health risks (Koube et al., 2022 ; Miller and Lillard, 2019). In 2013 alone, the global cost of corrosion was estimated to be $2.5 trillion, equivalent to 3.4% of the global GDP (NACE International, 2016). Thus, stringent mitigation practices are called for in order to reduce the impact of corrosion. In general, the most common approach to corrosion protection is achieved through coatings, which can be inorganic (e.g., chromates, zinc, cerium-based compounds) or organic (Cordeiro Neto et al., 2020; Li et al., 2023). Moreover, while corrosion is conventionally addressed through synthetic polymer coatings derived from petrochemical feedstocks that may contain hazardous components, these approaches remain non-renewable and environmentally persistent.

In response to growing concerns over climate change and energy security, biomass has emerged as a promising feedstock for biorefineries, offering a sustainable alternative to petroleum-based systems. Biomass is abundant, low-cost, and renewable, making it suitable for producing fuels, chemicals, and materials with lower environmental impact (Ashokkumar et al., 2022; Espro et al., 2021; Stevens, 2020). One example is lignocellulosic biomass, which consists primarily of cellulose, hemicellulose, and lignin –biopolymers of interest for renewable chemical production (Kobayashi and Fukuoka, 2013). Lignin is a complex aromatic polymer of phenylpropane units (Zakseski et al., 2010). Lignin in previous studies were used in different applications such as surfactants, adhesives, dispersants, packaging, and replacement for plastics due to its water impermeability, hydrophobicity, low-cost, and abundance. (Ang et al., 2019; Gendron et al., 2023; Miranda-Valdez et al., 2024; Zhou et al., 2015).

Rice, a staple food for over half the global population, is mainly consumed in Asian countries such as the Philippines, which produces large quantities of agricultural waste in the form of rice husk—the grain's outer layer. Due to its resistance to biodegradation, rice husk is often burned, releasing pollutants and respiratory irritants (El-Din Al-Mofty et al., 2023 ; Ramos et al., 2023). As a lignocellulosic biomass, rice husk remains underutilized despite its potential for biorefinery applications. Lignin can be extracted from rice husk source using deep eutectic solvent (DES) which are considered green alternatives to ionic liquids, offering similar solvating properties with lower toxicity and biodegradability. DES mixtures of choline chloride and p-toluene sulfonic acid mixture has been reported in the extraction of lignin from rice husk (Balasubramanian and

Quick Response Code	Access this article online	
	Website: www.mjsa.com.my	DOI: 10.26480/mjsa.02.2026.39.44

Cite The Article: Paler, K.M.S., Quimque, M.T.J., Bendoy, A.P. (2026). Valorization of Rice Husk Lignocellulose Via Microwave-Assisted Furan Functionalization and Its Corrosion Inhibition on Stainless Steel 304l. Malaysian Journal of Sustainable Agriculture (MJSA), 10(2): 39-44.

Venkatachalam, 2023). To the best of our knowledge, no study has yet explored lignin from other underutilized feedstock rice husk, nor has any research functionalized it using microwave-assisted approaches with bio-derived groups as a corrosion protection coating.

In this work, we propose a sustainable, microwave-assisted functionalization strategy to valorize lignocellulose from rice husk as green reactants, modifying DES-extracted rice husk lignin with additional corrosion-inhibiting groups, and investigating its corrosion-inhibiting performance on SUS304L stainless steel. This approach offers advantages in terms of reduced solvent use and energy consumption compared to conventional thermal synthesis.

2. Experimental Methods

2.1 Materials and Chemicals

Rice husk (RH) was sourced from a local rice mill in Cabadbaran, Agusan del Norte, Philippines. The husk was thoroughly washed, dried at 70°C for 24 hours, ground, and sieved. The chemicals used were supplied by Sigma-Aldrich Singapore and Thermo Fisher Scientific, including Aboslute Reagent (AR) dimethyl sulfoxide (DMSO), AR 1,4-dioxane, choline chloride ≥98%, p-toluenesulfonic acid monohydrate (pTSA) ≥98%, AR tetrahydrofuran (THF), tetraethylammonium chloride (TEAC) ≥98%, Aluminum chloride hexahydrate ≥99%, Ferric chloride hexahydrate ≥99%, and anhydrous sodium chloride ≥99%. SUS304L, consisting of a wt% composition of C 0.03, Cr 18.6, Ni 8.8, Mn 1.6, Si 0.5, N 0.09, P 0.006, and Fe balance, were used in the study and cut into 3 cm x 1 cm x 0.2 cm coupons.

2.2 Synthesis and Characterization of Deep Eutectic Solvent (DES)

DES was synthesized adapting the method of Balasubramanian and Venkatachalam. (Balasubramanian and Venkatachalam, 2023). Briefly, the DES was prepared by mixing choline chloride and *p*TSA in a 1:0.5 molar ratio at 50°C until a homogeneous liquid formed. The DES was characterized using FT-IR.

2.3 Rice Husk Pretreatment

Rice husk (15% w/w) was treated with DES at 80°C for 90 minutes. The resulting mixture was centrifuged, and the residue (RH residue) was collected. RH lignin (RH-L) was precipitated using distilled water, filtered, washed, and dried.

2.4 Microwave-Assisted Furan Functionalization of Rice Husk Lignin

RH residue was dissolved in a DMSO/TEAC mixture at 80°C, followed by the addition of $FeCl_3$ and RH lignin. The reaction proceeded at 110°C under microwave (Milestone RotoSYNTH Microwave Reactor) irradiation for 60 minutes. The functionalized RH-Lignin (fRH-L) was precipitated using distilled water, and then filtered, washed, and dried. Neat samples were analyzed for FT-IR (Thermo Scientific NICOLET iS5).

The lignin samples were acetylated for molecular weight determination via Gel Permeation Chromatography (GPC, Tosoh Eco SEC HLC-8420) and Pyrolysis-GasChromatography/Mass Spectroscopy (Py-GC/MS, Pyrolyzer + Agilent Technologies 7890B GC/MS). A 100 mg lignin sample was mixed with 3 mL of pyridine and 3 mL of acetic anhydride, stirred overnight at room temperature. The mixture was precipitated with 500 mL of distilled water to obtain the acetylated sample. The samples were dissolved in THF before injection for GPC analysis with polystyrene standards within a range of 9 to 600 kDA for calibration. Py-GC/MS was performed using a single-shot pyrolysis to 500 oC under Helium flow rate of 1.0 mL/min.

2.5 Corrosion Resistance Evaluation

Stainless steel 304L specimens were polished with 2000-1000# SiC sandpaper, degreased with acetone, sonicated with ethanol, dried, and applied via drop casting with a solution of 6 g/L lignin samples in dioxane, enough to fully cover the surface of the electrode. The samples were then heated at 120 °C for 30 minutes for annealing. Electrochemical tests were performed in 3.5 wt.% NaCl using a three-electrode setup with the stainless steel as the working electrode on a ZIVE MP1 Multichannel Electrochemical Workstation. A platinum wire and Ag/AgCl reference electrode were used as the counter and reference electrodes, respectively. Potentiodynamic Polarization (PDP) was performed at a scan rate of 0.5 mV/s and over a potential range of -0.25 to 0.25 V with respect to the open circuit potential (OCP) for each sample. After each measurement, the corrosion current density, i_{corr}, was determined from the linear region of the resulting Tafel diagram, which was proximal to the corrosion potential. Electrochemical Impedance Spectroscopy (EIS) was done over a frequency range of 100 kHz to 100 mHz, spaced logarithmically at 10 steps per decade, with a voltage signal amplitude of 20 mV and at OCP of each sample. EIS data was subsequently analyzed via AfterMath Electrochemical Studio.

3. Results And Discussion

3.1 Characterization

Lewis acid catalysis played a crucial role in the microwave-assisted functionalization of rice husk lignin. In this study, $AlCl_3$ and $FeCl_3$ were selected as catalysts based on their established use in biomass hydrolysis systems, particularly following the work of on glucose and cellulose hydrolysis (Du et al., 2023). The overall yield shown in **Table 1** of functionalized lignin increased with rising reaction temperature, whereas shorter reaction times resulted in lower yields, indicating the importance of sufficient thermal input. Catalyst identity also significantly influenced the reaction outcome wherein substituting $AlCl_3$ with $FeCl_3$ improved product yield under the tested conditions. In contrast, omitting the catalyst reduced the yield to 42%, a result that may reflect partial lignin depolymerization in the absence of Lewis acid mediation.

The functionalized rice husk lignin (RH-L) was produced from rice husk lignocellulose using a thermal energy-efficient microwave heating process. This strategy reduces the reaction time required by rapid and volumetric heating for chemical reactions compared to conventional techniques. A combination of molecular weight analysis and thermal degradation profiling supports the plausibility of 1,3,5,7-cyclooctatetraene (COT) formation from aromatic grafts despite the difficulty of structure confirmation in lignin systems (Dutta, 2024). Notably, the FTIR spectrum of the functionalized rice husk lignin (fRH-L), as shown in Figure. 1**,** revealed a decrease of guaiacyl (1030 cm^{-1}) and syringyl (1116 cm^{-1}) characteristic bands, alongside a reduction in C–H out-of-plane bending vibrations typical of para and ortho-substituted aromatics (812 and 682 cm^{-1}, respectively) (Balasubramanian and Venkatachalam, 2023). These changes in the FTIR spectra are consistent with substition on the aromatic rings, possibly due to furanic or carbohydrate-derived electrophilic substitution, as well as condensation reactions. A subsequent reduction in the broad O–H stretching (3350 cm^{-1}) further supports the formation of crosslinked or etherified structures which reduce hydroxyl content. Together, these FTIR findings suggest that the introduced moieties structurally modified the lignin macromolecule at both the aromatic and aliphatic levels.

Table 1: Percentage yield of microwave-assisted functionalization of rice husk lignin

Temperature (°C)	**Time** (minutes)	Catalyst	**%** Yield
90	60	$AlCl_3$	55
100	60	$AlCl_3$	57
110	60	$AlCl_3$	60
110	15	$AlCl_3$	50
110	30	$AlCl_3$	51
110	60	-	42
90	60	$FeCl_3$	51
100	60	$FeCl_3$	54
110	60	$FeCl_3$	64

Gel permeation chromatography (GPC) of acetylated lignin samples (Figure. 1B) revealed an increase in number-average molecular weight (Mn) from 932 to 1098 amu and in weight-average molecular weight (MW) from 3944 to 5104 amu following lignin modification, consistent with successful incorporation of additional functional moieties (Lakmini et al., 2024).

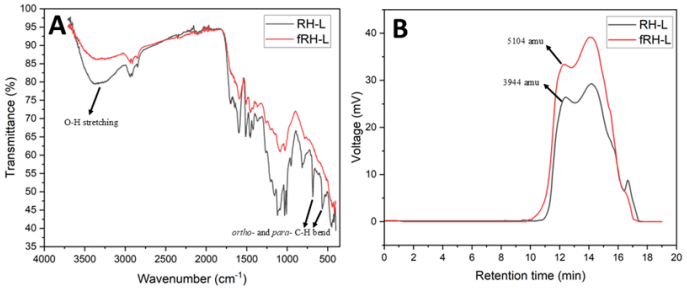

Figure 1: (A) FTIR and (B) GPC spectra of RH-L and fRH-L.

The Py-GC/MS chromatographs of the samples in Figure 2 reveal that upon pyrolysis at 500 °C under helium, fRH-L produced higher CO_2 relative to RH-L, suggesting the increase of oxygen heteroatoms and enhanced decarboxylation pathways, likely stemming from introduced carbohydrate- or furan-derived structures (Kawamoto, 2017). Relative to RH-L, the fRH-L exhibited a 61% increase in COT component area from 115,220.1 to 185,611.2 following pyrolysis. Moreover, the peak for 2-methoxyphenol disappears in fRH-L and is replaced by 1-(2-methyl-1-cyclopenten-1-yl)-ethanone. The disappearance of this lignin monomeric pyrolysis product indicates the introduction of furanic functional groups. Although not definitive, this pattern suggests a transformation pathway potentially enabled by the altered chemical structure of the modified lignin, consistent with enhanced generation of aromatic intermediates that may originate from thermally rearranged furanic structures introduced during grafting.

The acetylation step prior to pyrolysis enhances the volatility and interpretability of the chromatographic spectra by protecting labile hydroxyl groups. The acetylation of lignin produces COT and other thermally derived products, such as 1,4-dioxane-2,6-dione and acetic acid. The increase in the intensity of COT in Figure 2 indicates the probable increase in aromatic unsaturation and furanic content of fRH-L. Further investigation employing 2D NMR (e.g., HSQC) and isotopic labeling (e.g. ^{13}C-furfural) would further strengthen the responsible reaction mechanism.

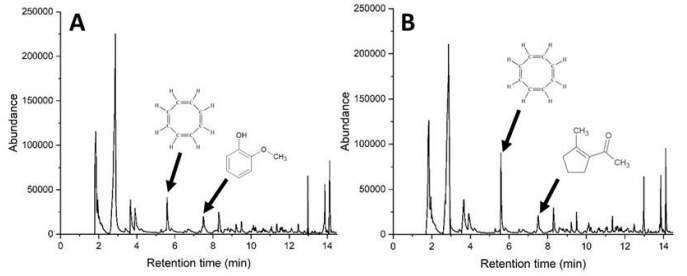

Figure 2: Py-GC/MS chromatograms of (A) RH-L and (B) fRH-L.

3.2 Anticorrosion Properties

The anticorrosion properties of RH-L and fRH-L were examined using EIS and PDP. For the EIS analysis, a corresponding circuit model composed of solution resistance, R_s, in series with a parallel combination of a Constant Phase Element, CPE, and a polarization resistance, R_p, was employed using AfterMath Electrochemical Studio software shown in Figure 3 to characterize the impedance spectrum. The equivalent circuit model employed to fit the EIS spectra is illustrated in Figure 3A and the obtained fitting data are presented in Table 2.

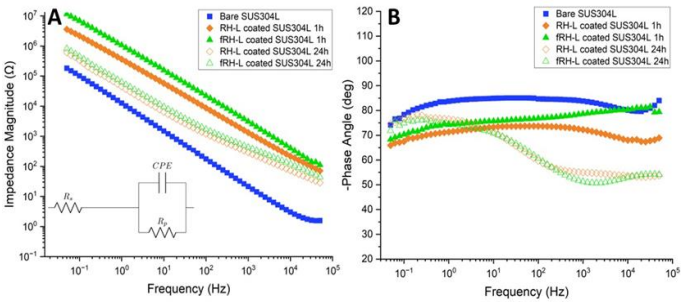

Figure 3: Bode plot diagrams of bare, RH-L coated, and fRH-L coated SUS304L steel in 3.5% NaCl solution. (A) Bode magnitude plot, and (B) Bode phase plot.

Table 2: Tafel Equivalent circuit model fitted parameters.

	R_s ($\Omega \cdot cm^2$)	CPE ($F \cdot cm^{-2}$)	CPE coefficient, α	R_p ($\Omega \cdot cm^2$)
Blank	17.82	7.26×10^{-5}	0.92	0.22×10^6
RH-L	15.72	2.90×10^{-6}	0.80	2.68×10^6
fRH-L	14.05	9.65×10^{-7}	0.85	1.66×10^7

To further elucidate the capacitive nature of the coatings, effective capacitance parameters (C_{eff}) and the distribution parameter (α) were derived from the Constant Phase Element (CPE) model in accordance with the graphical representation method proposed by Orazem and co-authors (Orazem et al., 2006). The following equation was used to calculate Q_{eff}:

$$Q_{eff} = \sin\left(\frac{\alpha\pi}{2}\right)\frac{-1}{Z'(2\pi f)^{\alpha}} \quad (1)$$

wherein Z' is the imaginary impedance magnitude, α is the CPE coefficient derived from the graphical representation method, and f is the corresponding frequency of the impedance measurement. The obtained values for the CPE coefficient and Q_{eff} are in good agreement with the equivalent circuit model fitted parameters. The α values were 0.87 (bare SUS304L), 0.80 (RH-L coated SUS304L), and 0.84 (fRH-L coated SUS304L), all of which indicate a high degree of capacitive behavior across all samples. The C_{eff} values show a similar trend with bare SUS304L (6.68×10^{-5} $F \cdot cm^{-2} \cdot s^{-0.13}$), higher than RH-L ($3.09 \times 10^{-6}$ $F \cdot cm^{-2} \cdot s^{-0.16}$) and fRH-L ($1.06 \times 10^{-6}$ $F \cdot cm^{-2} \cdot s^{-0.20}$). The lower capacitance of the fRH-L coating suggests the suppression of interfacial charge development which reduce the kinetics of charge-transfer processes associated with corrosion.

For the Bode magnitude plot, the magnitude at the low frequency can describe the anticorrosion ability of coatings (Christopher et al., 2016). The coated SUS304L exhibit a higher impedance, as shown in Figure 3A. At low frequencies, the impedance increased by approximately two orders of magnitude relative to the bare SUS304L, reaching 10^7 $\Omega \cdot cm^2$, which suggests that a relatively more effective barrier was produced through the addition of furanic moieties. This trend was also observed in a study on spin-coated beech and spruce lignin as corrosion inhibitors (Dastpak et al., 2018).

The α values after 24 hours were 0.91 (blank), 0.62 (RH-L), and 0.72 (fRH-L), while Qeff values increased notably for the coatings RH-L (9.20×10^{-5} $F \cdot cm^{-2} \cdot s^{-0.38}$) and fRH-L ($4.27 \times 10^{-5}$ $F \cdot cm^{-2} \cdot s^{-0.28}$), suggesting increased interfacial charge storage due to coating breakdown.

Potentiodynamic polarization conducted after 1 hour of immersion in 3.5% NaCl (Figure 5A) shows that the corrosion current density (i_{corr}) for the bare stainless steel was 190.2 $nA \cdot cm^{-2}$, equivalent to a corrosion rate of 2.0 x 10^{-3} mm/yr. Additionally, the RH-L and fRH-L coatings

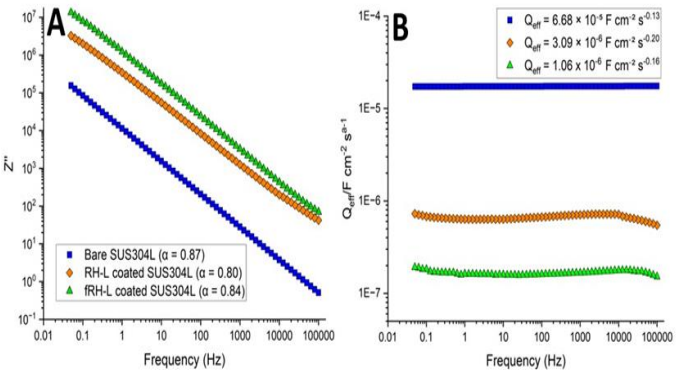

Figure 4: (A) Variation of the absolute value of the imaginary impedance magnitude and (B) effective CPE parameter Qeff as a function of frequency after 1 hour immersion in 3.5% NaCl.

reduced the bare stainless steel icorr to 5.7 nA·cm^{-2} (6.0 x 10^{-5} mm/yr) and 2.7 nA·cm^{-2} (1.1 x 10^{-6} mm/yr), corresponding to corrosion inhibition efficiencies of 97% and 99%, respectively. These results are in line with or exceed those of other lignin-based coating systems such as lignosulfonate-ZnO/polyurethane composites (~98%) and termite frass lignin-based coatings (~70%) (Hussin et al., 2014 ; Kulkarni et al., 2021).

Moreover, Tafel analysis at 24 hours showed lower corrosion current density for fRH-L (11.9 nA·cm^{-2}) compared to RH-L (39.0 nA·cm^{-2}) and the bare metal (36.1 nA·cm^{-2}), equivalent to 67% and -7.4% inhibition efficiency, respectively. The fRH-L retains a level of protection over extended exposure.

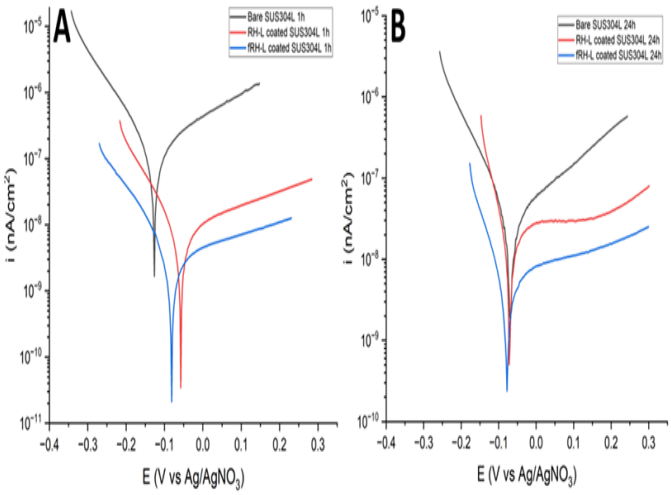

Figure 5: Potentiodynamic polarization curves of bare, RH-L-coated sample, fRH-L-coated sample SUS304L after (A) 1 hour and (B) 24 hours immersion in 3.5% NaCl solution.

Based on the Potentiodynamic polarization curves in Figure 5, a marked reduction in current density across both the anodic and cathodic branches for lignin-coated stainless steel, relative to the uncoated metal. Previous investigations have shown that lignin acts as a dual-function inhibitor, simultaneously suppressing anodic metal dissolution and retarding cathodic oxygen reduction, even when present in low concentrations in corrosive environments (Akbarzadeh et al., 2011; Hussin et al., 2014 ; Shivakumar et al., 2017). For instance, organosolv lignin at concentrations as low as 500 ppm has been shown to have inhibition efficiencies of up to 98%, primarily attributed to its antioxidant functionality and the electrostatic adsorption of protonated lignin molecules onto the metal surface. These interactions impede chloride ion adsorption and promote the formation of protective ferric–lignin complexes through coordination with phenolic hydroxyl groups, thereby enhancing charge transfer resistance (Akbarzadeh et al., 2011).

The reduction of electrochemical activity reflects the uniform influence of the lignin layer, supporting the interpretation of a mixed-mode inhibition mechanism. In the case of SUS304L stainless steel exposed to 3.5% NaCl, the dominant electrochemical reactions include the cathodic reduction of dissolved oxygen ($O_2 + 2H_2O + 4e^- \rightarrow 4OH^-$) and the anodic dissolution of alloying elements such as Fe, Ni, and Cr ($M \rightarrow M^{n+} + ne^-$) (Alonso-Falleiros and Wolynec, 2022). The observed decrease in activity for both half-reactions suggests that the lignin-based coatings can interfere with interfacial redox processes, consistent with a mixed-mode inhibition mechanism.

The SEM micrographs shown in Figure 6 provided insight into the surface morphology and degradation behavior of bare and lignin-coated SUS304L before and after exposure to 3.5 wt.% NaCl. The uncoated SUS304L exhibit linear surface defects from polishing with SiC emery papers. In contrast, both RH-L and fRH-L coated SUS304L revealed the presence of surface cracks within the deposited lignin layers. The RH-L coating exhibited longer and more continuous cracks (Figure 6C). At the same time, fRH-L film showed a higher density of microcracks (Figure 6E), suggesting differences in film formation and mechanical integrity.

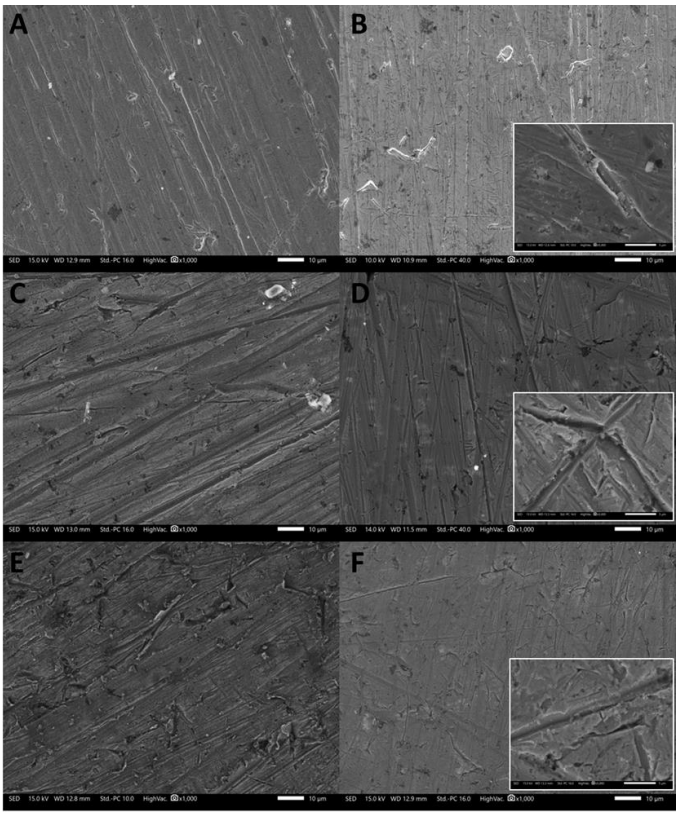

Figure 6: SEM micrographs of (A, B) bare SUS 304L, (C, D) RH-L coated SUS 304L, and (E, F) fRH-L coated SUS 304L before and after 24 h exposure to 3.5 wt.% NaCl. All main images were acquired at 1,000× magnification, with post-exposure images including insets at 5,000× magnification.

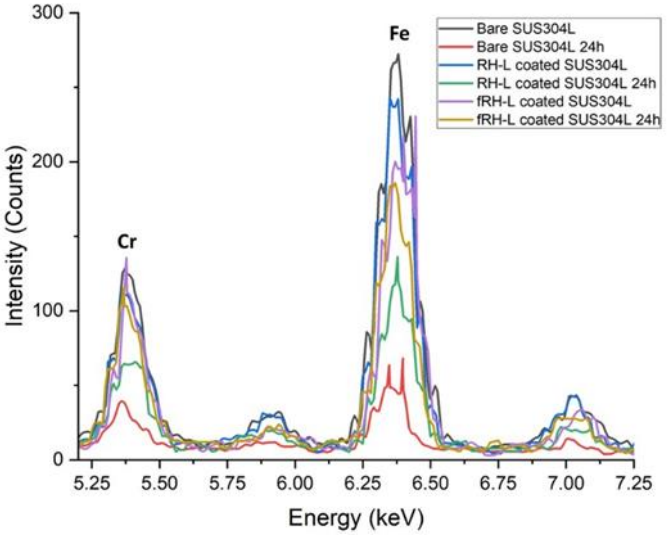

Figure 7: EDX analysis of bare SUS304L before and after 24h exposure to 3.5% NaCl.

After 24 hours of immersion (Figure 7), a marked decrease of intensity for Fe and Cr in the EDX analysis in bare SUS304L was observed with chloride-induced pitting corrosion (Figure 6B). The Bode magnitude plots (see Figure 3) show a decrease in impedance and phase angle responses at medium to high frequencies for both coated samples after 24 hours of immersion. These shifts indicate delamination or water ingress, reducing the dielectric integrity of the films.

The contact angle measurements are 67°, 81°, and 87° for the bare SUS304L, RH-L coated SUS304L, and fRH-L coated SUS304L, respectively. These findings support the increased crosslinking density, barrier functionality, and reduced wettability in chloride-rich environments of the lignin-based systems. Despite microcracks in the surface of fRH-L, the resulting reduction in the hydrophilicity within the polymer matrix limits the diffusion of corrosive electrolytes, limiting moisture and ion ingress. Additionally, the elevated oxygen content observed in the thermal

degradation profiles in Figure 2 suggests the presence of moieties that may contribute to improved adhesion through hydrogen bonding or coordination between the coating and the metal surface (Espro et al., 2021; Dastpak et al., 2018).

The polarization resistance of the coatings in this study is shown in Table 3 together with lignin-based corrosion-resistant coatings previously reported. The Rp of fRH-L (1.7×10^7 Ω·cm^2) is higher than that of the RH-L coating (7.7×10^6 Ω·cm^2) and bare SUS304L (2.2×10^5 Ω·cm^2), which demonstrates the enhanced corrosion resistance through functionalization of rice husk lignin. Furthermore, the Rp of the lignin coatings in this study shows comparable values to those of other reported corrosion-resistant coatings, without the use of petroleum-based compositing or crosslinking.

Table 3: Comparison of Rp Values from this Study and other Reported Lignin-based Coating Systems

Coating system	Metal Substrate	Electrolyte Concentration	Coating system R_p (Ω·cm^2)	Substrate R_p (Ω·cm^2)	Reference
RH-L	SUS304L	3.5 % NaCl	7.7×10^6	2.2×10^5	This study
fRH-L	SUS304L	3.5 % NaCl	1.7×10^7	2.2×10^5	This study
ZnO-Lignosulfonate nanocomposite	Mild Steel	3.5 % NaCl	3.6×10^3	2.0×10^2	Christopher et al., 2016
Termite Frass Lignin-epoxy	Carbon steel	0.5 M NaOH	4.4x10	1.3 x10	Kulkarni et al., 2021
Lignin-polydimethyl-siloxane	Carbon steel	1 M NaCl	3.0×10^{10}	-	Wang, et al., 2024
Kraft Lignin	Iron Phosphated Steel	5 % NaCl	1.5×10^5	1.9×10^3	Dastpak et al., 2020

4. Conclusion

This study demonstrates the valorization of rice husk lignocellulose through a sustainable microwave-assisted functionalization strategy, which modifies DES-extracted rice husk lignin with furanic moieties. The study also evaluates its potential as a corrosion-inhibiting coating for SUS304L stainless steel. Structural characterization (FTIR, GPC, and Pyrolysis-GC/MS) confirmed an increase in molecular weight and aromatic density of fRH-L. The Potentiodynamic Polarization curve of fRH-L has shown a mixed-mode inhibition mechanism, suppressing both anodic and cathodic reactions. Electrochemical measurements revealed a corrosion inhibition efficiency of up to 99% and a corrosion rate of 1.1 x 10^{-6} mm/yr, with excellent agreement between EIS- and Tafel-derived corrosion current densities. EIS and PDP measurements after 24 hours of exposure to 3.5% NaCl, obtained from SUS304L and coated surfaces, demonstrated the higher protection capability of fRH-L at a 67% inhibition efficiency. This finding indicates the applicability of functionalization using other lignocellulosic biomass for the development of corrosion inhibitors. Overall, while rigorous long-term stability assessments in industrially relevant conditions remain necessary, this work establishes a foundation for the development of sustainable coatings for corrosion protection.

Authorship Contributions

CrediT authorship contribution statement: Karl Michael S. Paler: Writing – original draft, Visualization, Validation, Methodology, Investigation, Formal analysis, Data curation, Conceptualization. Mark Tristan Quimque: Writing – original draft, Supervision. Anelyn P. Bendoy: Writing – original draft, Visualization, Supervision, Formal analysis, Data curation. All authors have read and agreed to the published version of the manuscript.

Acknowledgement

This research was supported by the Department of Science and Technology–Accelerated Science and Technology Human Resource Development Program (DOST-ASTHRDP)

References

Akbarzadeh, E., Ibrahim, M. N. M., and Rahim, A. A., 2011. Corrosion Inhibition of Mild Steel in Near Neutral Solution by Kraft and Soda Lignins Extracted from Oil Palm Empty Fruit Bunch. International `Journal of Electrochemical Science, 6(11), Pp. 5396–5416. https://doi.org/10.1016/s1452-3981(23)18416-1

Alonso-Falleiros, N., and Wolynec, S., 2002. Correlation between Corrosion Potential and Pitting Potential for AISI 304L Austenitic Stainless Steel in 3.5% NaCl Aqueous Solution. Materials Research, 5(1), Pp. 77–84. https://doi.org/10.1590/s1516-14392002000100013

Ang, A. F., Ashaari, Z., Lee, S. H., Md Tahir, P., and Halis, R., 2019. Lignin-based copolymer adhesives for composite wood panels – A review. International Journal of Adhesion and Adhesives, 95, 102408. https://doi.org/10.1016/j.ijadhadh.2019.102408

Ashokkumar, V., Venkatkarthick, R., Jayashree, S., Chuetor, S., Dharmaraj, S., Kumar, G., Chen, W.-H., and Ngamcharussrivichai, C., 2022. Recent advances in lignocellulosic biomass for biofuels and value-added bioproducts - A critical review. Bioresource Technology, 344, 126195. https://doi.org/10.1016/j.biortech.2021.126195

Baddoo, N. R., 2008. Stainless steel in construction: A review of research, applications, challenges and opportunities. Journal of Constructional Steel Research, 64(11), Pp. 1199–1206. https://doi.org/10.1016/j.jcsr.2008.07.011

Balasubramanian, S., and Venkatachalam, P., 2023. Valorization of rice husk agricultural waste through lignin extraction using acidic deep eutectic solvent. Biomass and Bioenergy, 173, 106776. https://doi.org/10.1016/j.biombioe.2023.106776

Biomass Conversion and Sustainable Biorefinery. 2024. In M. A. R., Lubis, S. H., Lee, E., Mardawati, S., Rahimah, P., Antov, R., Andoyo, Ľ., Krišťák, and B. Nurhadi (Eds.). Green Energy and Technology. Springer Nature Singapore. https://doi.org/10.1007/978-981-99-7769-7

Christopher, G., Kulandainathan, M. A., and Harichandran, G., 2016. Biopolymers nanocomposite for material protection: Enhancement of corrosion protection using waterborne polyurethane nanocomposite coatings. Progress in Organic Coatings, 99, Pp. 91–102. https://doi.org/10.1016/j.porgcoat.2016.05.012

Cordeiro Neto, A. G., Pellanda, A. C., de Carvalho Jorge, A. R., Floriano, J. B., and Coelho Berton, M. A., 2020. Preparation and evaluation of corrosion resistance of a self-healing alkyd coating based on microcapsules containing Tung oil. Progress in Organic Coatings, 147, 105874. https://doi.org/10.1016/j.porgcoat.2020.105874

Dastpak, A., Hannula, P.-M., Lundström, M., and Wilson, B. P., 2020. A sustainable two-layer lignin-anodized composite coating for the corrosion protection of high-strength low-alloy steel. Progress in Organic Coatings, 148, 105866. https://doi.org/ 10.1016/ j.porgcoat. 2020.105866

Dastpak, A., Yliniemi, K., De Oliveira Monteiro, M. C., Höhn, S., Virtanen, S., Lundström, M., and Wilson, B. P., 2018. From Waste to Valuable Resource: Lignin as a Sustainable Anti-Corrosion Coating. Coatings, 8(12), 454. https://doi.org/10.3390/coatings8120454

Du, Q., Guo, X., Zhu, H., Cheng, Y., Wang, L., and Li, X., 2023. One-pot conversion of cellulose to HMF under mild conditions through decrystallization and dehydration in dimethyl sulfoxide/ tetraethylammonium chloride. Chemical Engineering Journal, 475, 146217. https://doi.org/10.1016/j.cej.2023.146217

Dutta, S., 2024. Catalytic Transformation of Carbohydrates into Renewable Organic Chemicals by Revering the Principles of Green Chemistry. ACS Omega, 9(25), Pp. 26805–26825. https://doi.org/10.1021/ acsomega. 4c01960

El-Din Al-Mofty, S., Elghazawy, N. H., and Azzazy, H. M. E., 2023. A one-step facile process for extraction of cellulose from rice husk and its use for mechanical reinforcement of dental glass ionomer cement. RSC Sustainability, 1(7), Pp. 1743–1750. https://doi.org/10.1039/ d3su 00230f

Espro, C., Paone, E., Mauriello, F., Gotti, R., Uliassi, E., Bolognesi, M. L., Rodríguez-Padrón, D., and Luque, R., 2021. Sustainable production of pharmaceutical, nutraceutical and bioactive compounds from biomass and waste. Chemical Society Reviews, 50(20), Pp. 11191–11207. https://doi.org/10.1039/d1cs00524c

Gendron, J., Bruel, C., Boumghar, Y., and Montplaisir, D., 2023. Preparation and optimization of a lignin-based pressure-sensitive adhesive. MethodsX, 10, 102144. https://doi.org/10.1016/j.mex.2023.102144

Haruna, K., and Saleh, T. A., 2022. Graphene oxide with dopamine functionalization as corrosion inhibitor against sweet corrosion of X60 carbon steel under static and hydrodynamic flow systems. Journal of Electroanalytical Chemistry, 920, 116589. https://doi.org/10.1016/ j.jelechem.2022.116589

Hussin, M. H., Shah, A. M., Rahim, A. A., Ibrahim, M. N. M., Perrin, D., and Brosse, N., 2014. Antioxidant and anticorrosive properties of oil palm frond lignins extracted with different techniques. Annals of Forest Science, 72(1), Pp. 17–26. https://doi.org/10.1007/s13595-014-0405-1

Kawamoto, H., 2017. Lignin pyrolysis reactions. Journal of Wood Science, 63(2), Pp. 117–132. https://doi.org/10.1007/s10086-016-1606-z

Kobayashi, H., and Fukuoka, A., 2013. Synthesis and utilisation of sugar compounds derived from lignocellulosic biomass. Green Chemistry, 15(7), 1740. https://doi.org/10.1039/c3gc00060e

Koube, K. D., Kennedy, G., Bertsch, K., Kacher, J., Thoma, D. J., and Thadhani, N. N., 2022. Spall damage mechanisms in laser powder bed fabricated stainless steel 316L. Materials Science and Engineering: A, 851, 143622. https://doi.org/10.1016/j.msea.2022.143622

Kulkarni, P., Ponnappa, C. B., Doshi, P., Rao, P., and Balaji, S., 2021. Lignin from termite frass: a sustainable source for anticorrosive applications. Journal of Applied Electrochemistry, 51(10), Pp. 1491–1500. https://doi.org/10.1007/s10800-021-01592-8

Lakmini, L. M. N., Deshan, A. D. K., Bartley, J., Rackemann, D., and Moghaddam, L., 2024. One pot synthesis of furan-modified lignin from agricultural waste via lignin-first approach. Bioresource Technology, 401, 130728. https://doi.org/10.1016/j.biortech.2024.130728

Li, P., Zhang, Z., Zhang, X., Li, K., Jin, Y., and Wu, W., 2023. DES : their effect on lignin and recycling performance. In RSC Advances (Vol. 13, Issue 5, Pp. 3241–3254). Royal Society of Chemistry (RSC). https:// doi.org/10.1039/d2ra06033g

Li, W., Zhang, S., He, D., Cai, M., He, C., and Fan, X., 2023. Ti3C2@ZnO-reinforced interpenetrating polymer network coating toward harsh wear/corrosion protection. Tribology International, 188, 108877. https://doi.org/10.1016/j.triboint.2023.108877

Loto, R. T., 2019. Comparative study of the pitting corrosion resistance, passivation behavior and metastable pitting activity of NO7718, NO7208 and 439L super alloys in chloride/sulphate media. Journal of Materials Research and Technology, 8(1), Pp. 623–629. https://doi.org/10.1016/j.jmrt.2018.05.012

Miller, D. M., and Lillard, R. S., 2019. An Investigation into the Stages of Alloy 625 Crevice Corrosion in an Ocean Water Environment: Initiation, Propagation and Repassivation in a Remote Crevice Assembly. Journal of The Electrochemical Society, 166(11), C3431–C3442. https://doi.org/10.1149/2.0491911jes

Miranda-Valdez, I. Y., Mäkinen, T., Hu, X., Lejon, J., Elamir, M., Viitanen, L., Jannuzzi, L., Koivisto, J., and Alava, M. J., 2024. Bio-Based Foams to Function as Future Plastic Substitutes by Biomimicry: Inducing Hydrophobicity with Lignin. Advanced Engineering Materials, 26(20). https://doi.org/10.1002/adem.202400233

NACE International. 2016. International measures of prevention, application, and economics of corrosion technologies (IMPACT). NACE International. https://impact.nace.org

Orazem, M. E., Pébère, N., and Tribollet, B., 2006. Enhanced Graphical Representation of Electrochemical Impedance Data. Journal of The Electrochemical Society, 153(4), B129. https://doi.org/10.1149/1. 2168377

Ramos, M., Laveriano, E., San Sebastián, L., Perez, M., Jiménez, A., Lamuela-Raventos, R. M., Garrigós, M. C., and Vallverdú-Queralt, A., 2023. Rice straw as a valuable source of cellulose and polyphenols: Applications in the food industry. Trends in Food Science & Technology, 131, Pp. 14–27. https://doi.org/10.1016/j.tifs.2022.11.020

Shivakumar, M., Dharmaprakash, M. S., Manjappa, S., and Nagashree, K. L., 2017. Corrosion Inhibition Performance of Lignin Extracted from Black Liquor on Mild Steel in 0.5 M H2SO4 Acidic Media. Portugaliae Electrochimica Acta, 35(6), Pp. 351–359. https://doi.org/10.4152/ pea.201706351

Stevens, E. S., 2020. Green Plastics. Princeton University Press. https://doi.org/10.2307/j.ctv10crf29

Wang, H., Pu, Y., Ragauskas, A., Yang, B., From Lignin to Valuable Products Strategies, Challenges, and Prospects, Bioresour. Technol. 271 2019, Pp. 449–461. https://doi.org/10.1016/j.biortech.2018.09.072.

Wang, J., Seidi, F., Shi, X., Li, C., Huang, Y., and Xiao, H., 2025. Unveiling the potential of dual-extrinsic/intrinsic self-healing lignin-based coatings for anticorrosion applications. International Journal of Biological Macromolecules, 285, 138073. https://doi.org/10.1016/ j.ijbiomac. 2024.138073

Zakzeski, J., Bruijnincx, P. C. A., Jongerius, A. L., and Weckhuysen, B. M., 2010. The Catalytic Valorization of Lignin for the Production of Renewable Chemicals. Chemical Reviews, 110(6), Pp. 3552–3599. https://doi.org/10.1021/cr900354u

Zhou, M., Wang, W., Yang, D., and Qiu, X., 2015. Preparation of a new lignin-based anionic/cationic surfactant and its solution behaviour. RSC Advances, 5(4), Pp. 2441–2448. https://doi.org/10.1039/c4ra10524a